

Towards a Predictive Capability for Local Helicity Injection Startup

J. L. Barr
on behalf of the PEGASUS Team



University of
Wisconsin-Madison

56th American Physical Society
Division of Plasma
Physics Meeting

New Orleans, LA
Oct. 28th, 2014

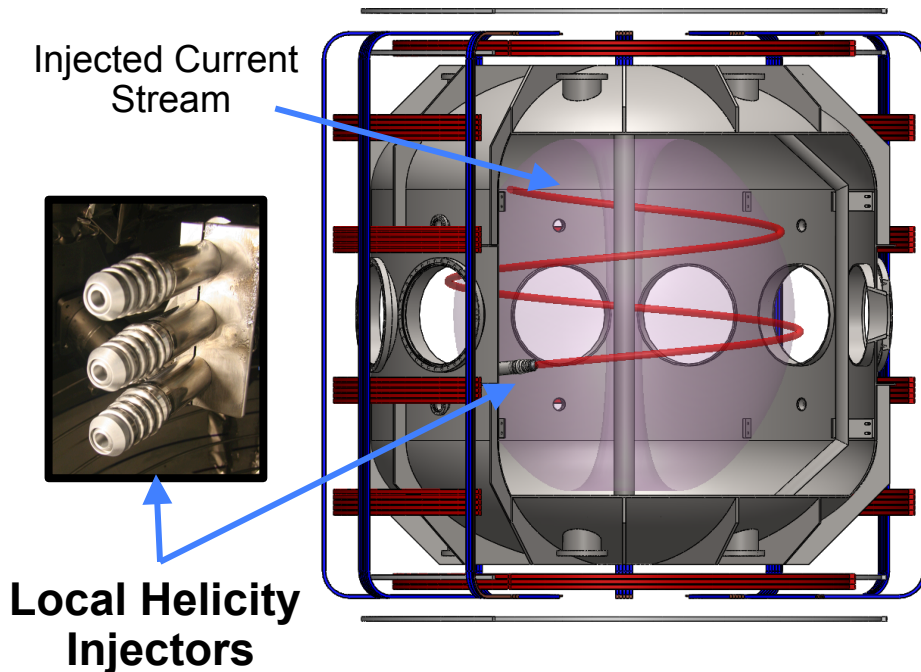


PEGASUS
Toroidal Experiment

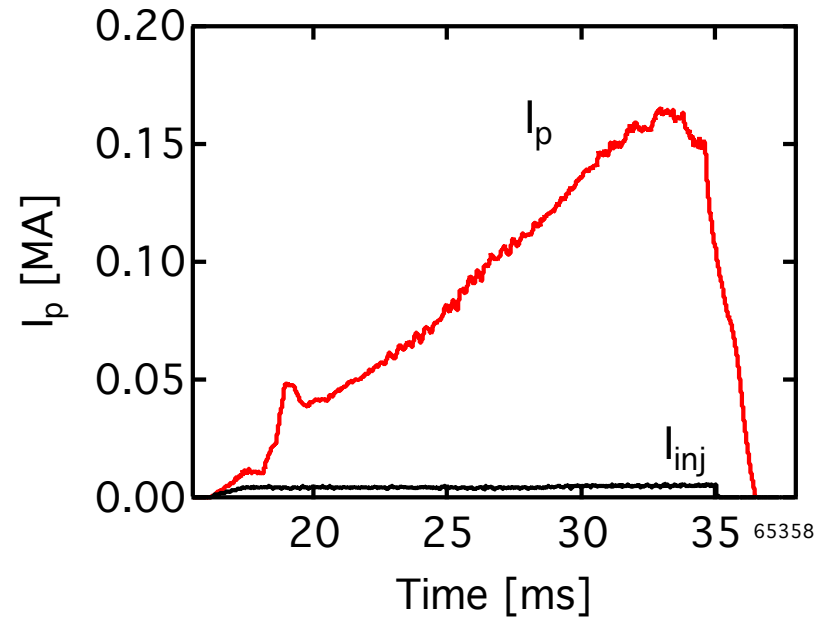


Local Helicity Injection (LHI) is a Promising Non-Solenoidal Startup Technique

Current injected on outboard side



$I_p \leq 0.18 \text{ MA}$ ($I_{inj} = 5 \text{ kA}$)



- Unstable current streams form tokamak-like state via Taylor relaxation
- Appears scalable to MA-class startup

A Hierarchy of Predictive Models Being Developed for LHI Startup



1. Maximum I_p limits*

Taylor Relaxation

$$I_p \leq I_{TL} \sim \sqrt{\frac{I_{TF} I_{inj}}{w}}$$

Helicity Conservation

$$V_{LHI} \approx \frac{A_{inj} B_{\phi, inj}}{\Psi} V_{inj}$$

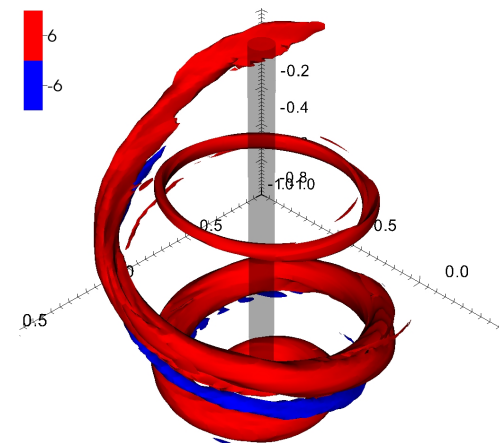
2. 0-D power-balance $I_p(t)$

$$I_p [V_{LHI} + V_{IR} + V_{IND}] = 0; \quad I_p \leq I_{TL}$$

3. 3D Resistive MHD (NIMROD)**

– See Sovinec, GP8.00047

Simulated current stream reconnection in NIMROD



*D.J. Battaglia, et al. *Nucl. Fusion* **51** (2011) 073029.

*N.W. Eidietis, Ph.D. Thesis, UW-Madison, 2007.

**J. O'Bryan, Ph.D. Thesis, UW-Madison, 2014.

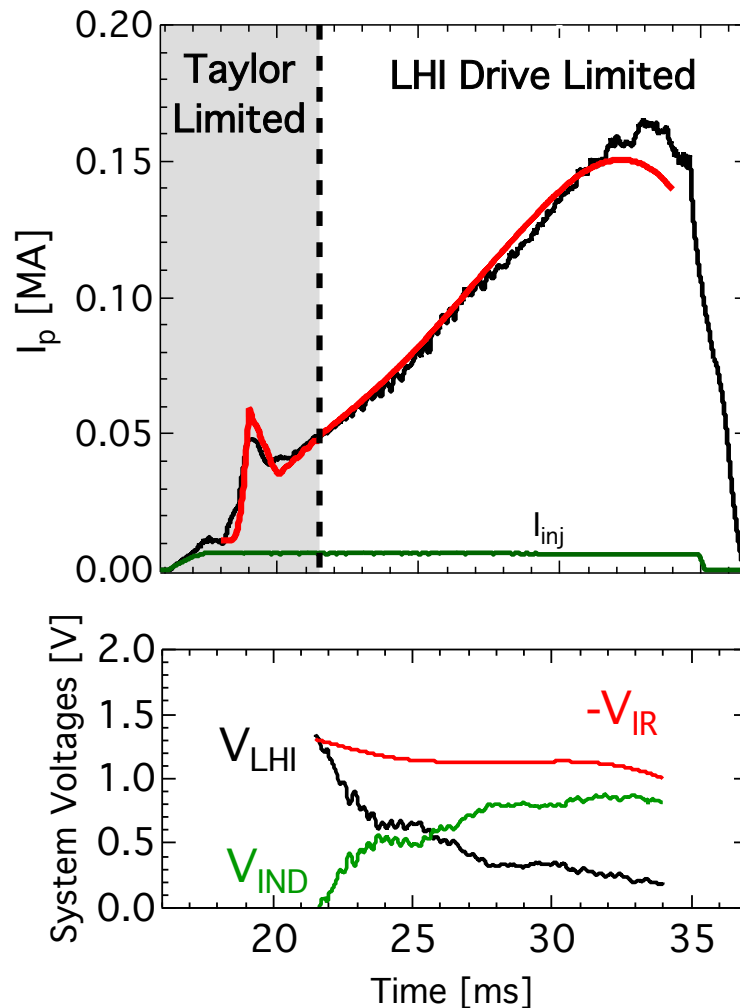
J. O'Bryan, C.R. Sovinec, *Plasma Phys. Control. Fusion* **56 064005 (2014)



2. 0-D Power-Balance: Lumped-Parameter Model for Predictive $I_p(t)$

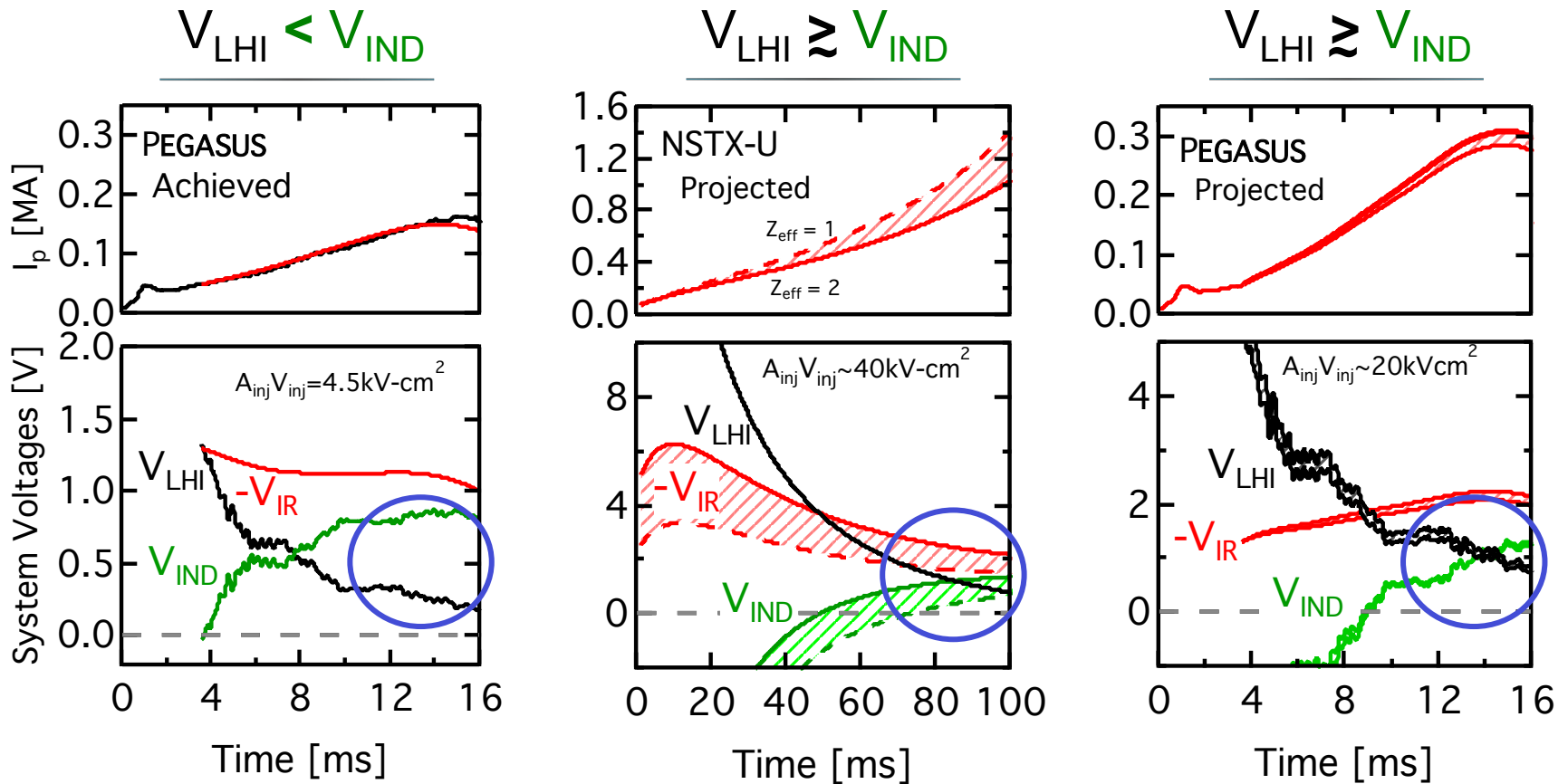
- Model elements:
 - Inputs: $R_0(t)$, $\text{shape}(t)$, $V_{\text{LHI}}(t)$, $\eta(t)$, $\ell_i(t)$
 - Low- A inductance, force-balance
- Reasonable agreement between calculated $I_p(t)$ and measurement
- High- I_p : current drive dominated by PF induction, geometry evolution

0-D model predictions vs data





Physics Test for MA Startup on NSTX-U Requires Increased Helicity Injection Drive

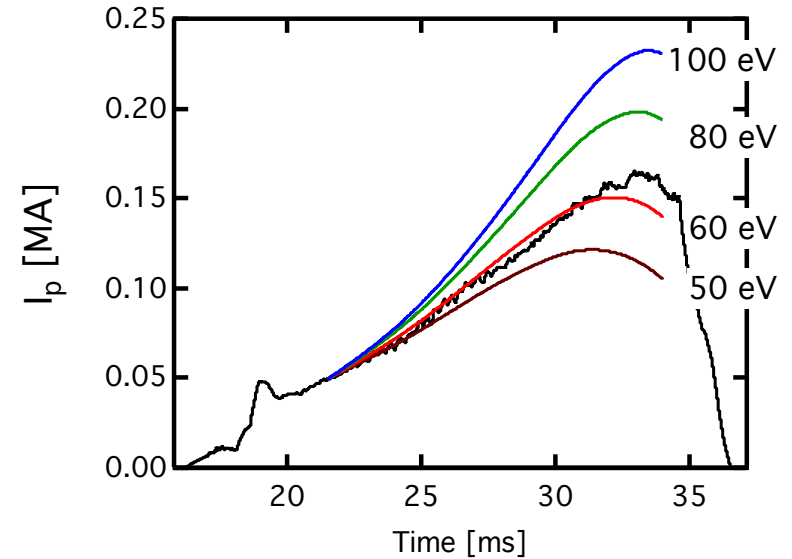


- Confinement when $V_{LHI} \gtrsim V_{IND}$ is a critical issue
 - At $I_p \sim 0.2-0.3$ MA in PEGASUS



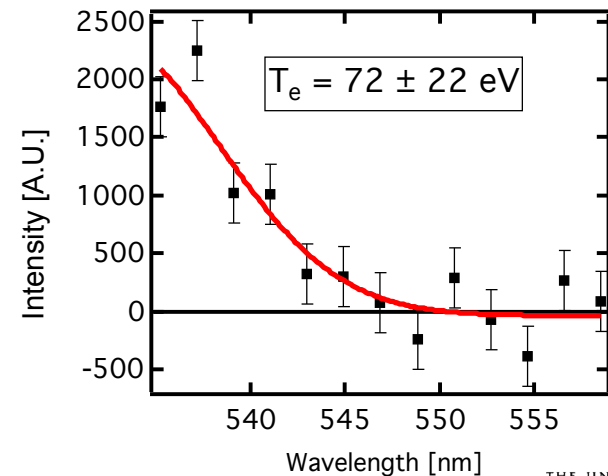
Knowledge of Confinement an Important Question for Predictability

- $I_p(t)$ model depends critically on η
 - Initial Thomson scattering: $T_e(0) \sim 70$ eV



- Dual confinement regimes?

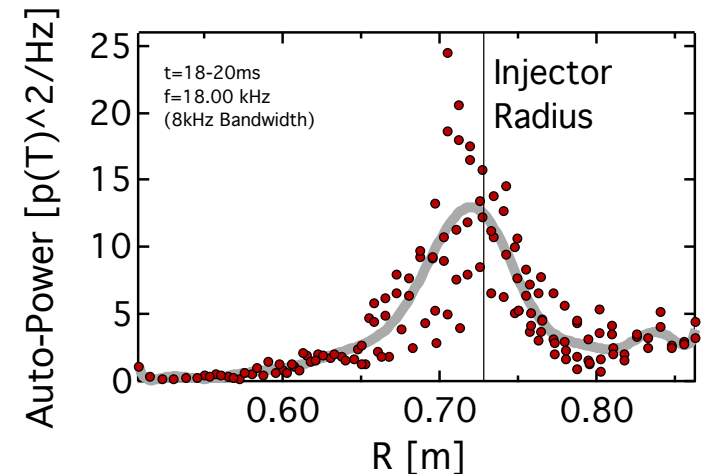
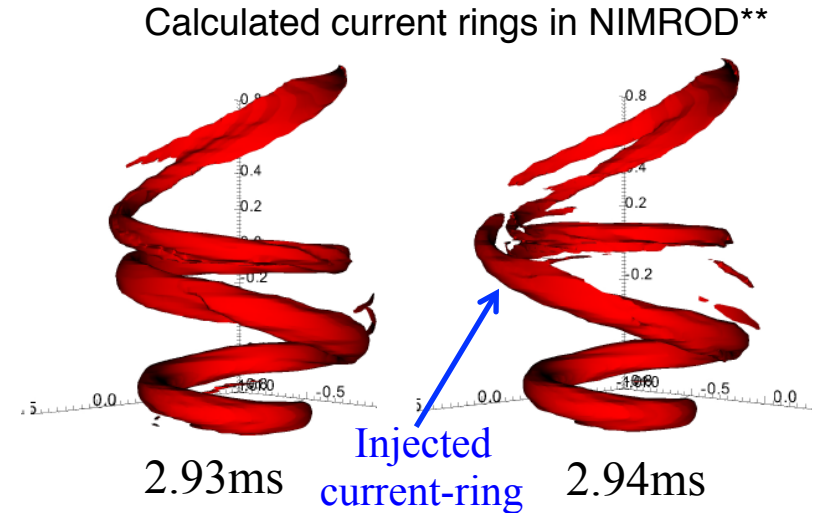
| Warm Core | Cool Edge |
|-------------------|---------------------|
| OH-like | Stochastic |
| Inductive drive | Reconnection |
| Low \tilde{B}/B | Large \tilde{B}/B |






3. NIMROD Simulations Show I_p Growth Resulting from Reconnection in Edge

- Resistive MHD modeling (NIMROD)
- Divertor injection
 - Coherent current streams reconnect
 - Inject current rings
- Qualitative agreement to experiment:
 - Injector-localized MHD
 - Intermittent MHD bursts
 - $\Delta I_p \sim I_{inj}$ jumps
 - Reconnection driven anomalous ion heating observed (M.G. Burke, PP8.00095)



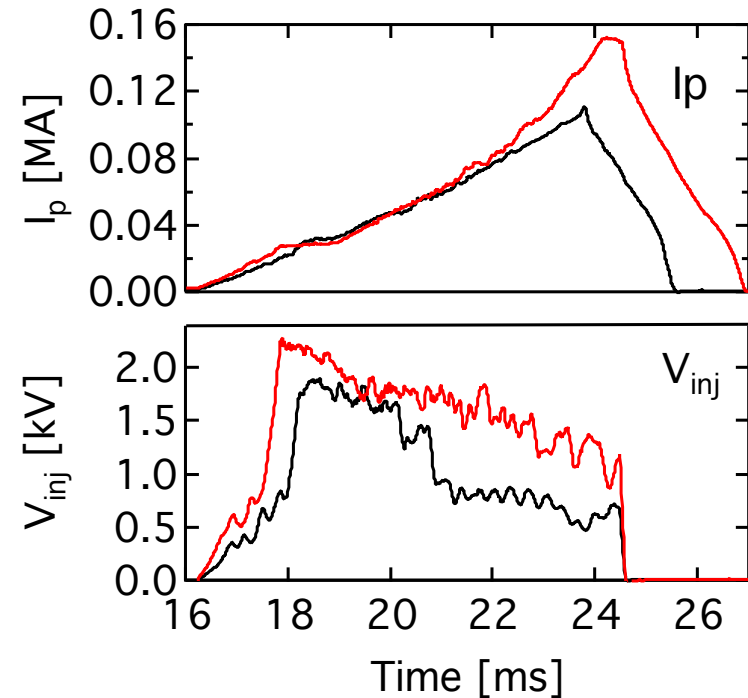
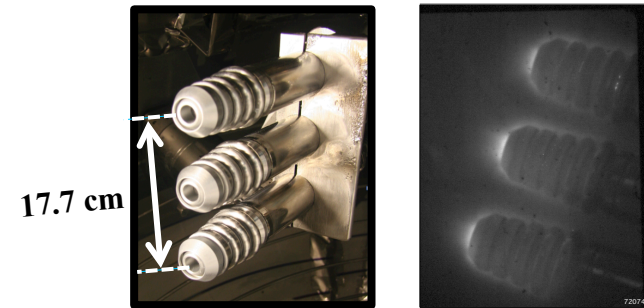


Understanding Injector Physics Enables High V_{inj} Operation

- High-power, low-PMI while **immersed in scrape-off plasma**
 - Cathode shaping mitigates cathode spots
 - Shield rings, local limiter prevent arc-back
- I_p increases with V_{inj} 
- J_{inj} , V_{inj} depend on tokamak scrape-off density
 - Space-charge neutralization of streams

$$J_{INJ} = n_{edge} e \sqrt{\frac{2e}{m_e}} \sqrt{V_{INJ}}$$

Advanced injectors with quiescent operation



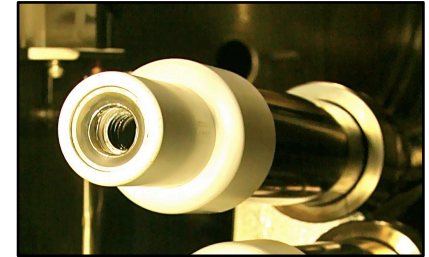


Technology & Science Challenges for NSTX-U & Beyond

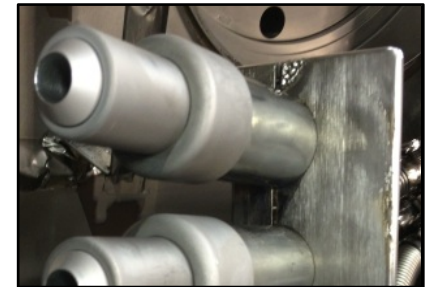
- Long-pulse startup (0.1 s)
 - Injector heat load
 - Edge density control
 - Plasma control
- High B_{TF}
 - Confinement scaling
 - Effective injector size
 - Initial tokamak formation
 - Reconnection with high guide field
- Plasma size scaling
- Close fitting wall
 - Potentially complicates relaxation

Injector technology evolving to meet physics challenges

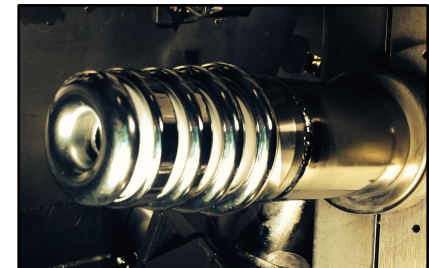
Concave cathode



**Frustum cathode,
local limiter**



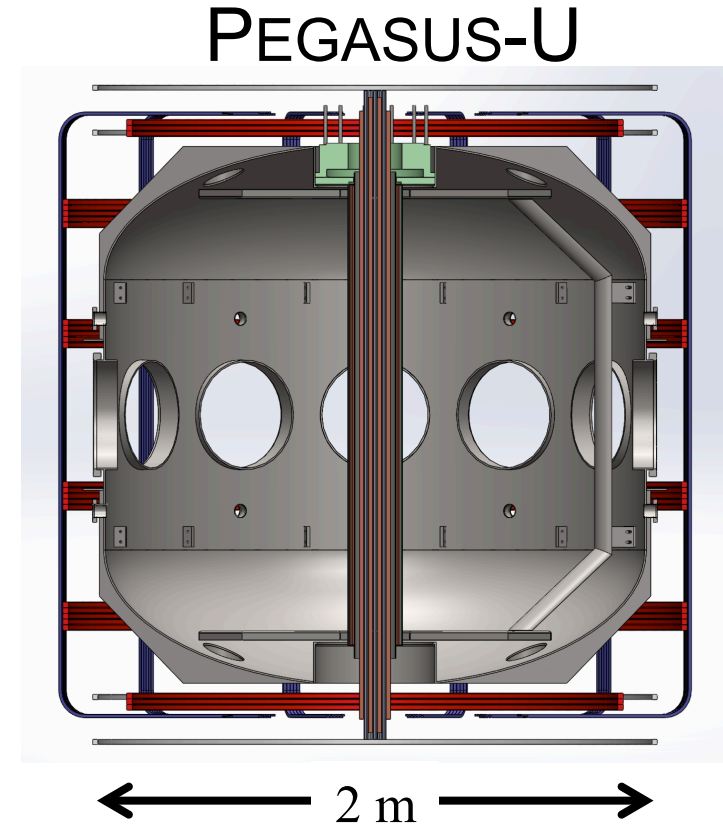
**High heat-flux
cathode,
shield rings**





PEGASUS-U to Address Physics, Technology for Scalable LHI Startup

- Long pulse startup (0.1 s)
- New central column ($A \sim 1.2$)
 - Increased B_{TF} (5x)
 - New OH solenoid, PPPL (6x V-s)
- Enhanced divertor coils
- Upgraded High- V_{LHI} Injectors
 - Remotely insertable
- Core diagnostics:
 - Multipoint TS
 - CHERS via DNB
- Supporting the 5 year plan for NSTX-U





Moving Towards Predictable, MA-Class, Non-Solenoidal Startup

- A hierarchy of models is being developed for LHI startup:
 - Max I_p : helicity conservation, Taylor relaxation
 - $I_p(t)$: 0-D power-balance (future: TSC)
 - Detailed dynamics: resistive MHD (NIMROD)
- Outstanding issues:
 - Scaling to high toroidal field, longer-pulse, large size
 - Confinement, stability in LHI drive dominant regime
 - Edge density, J_{inj} control strategies
 - Advanced injector development
- PEGASUS-U will address critical LHI physics issues for NSTX-U

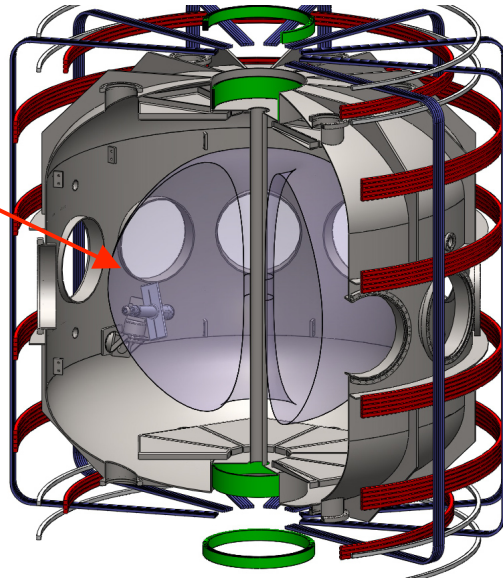
K.E. Thome talk: next this session, GO3
PEGASUS group posters: session PP8



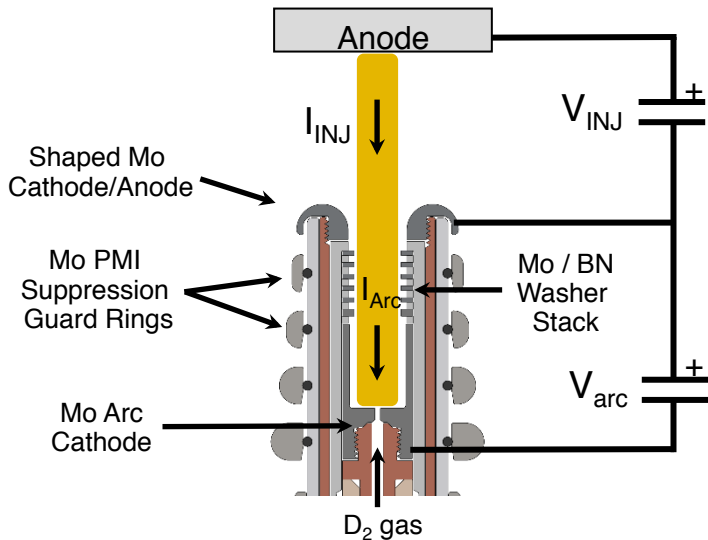
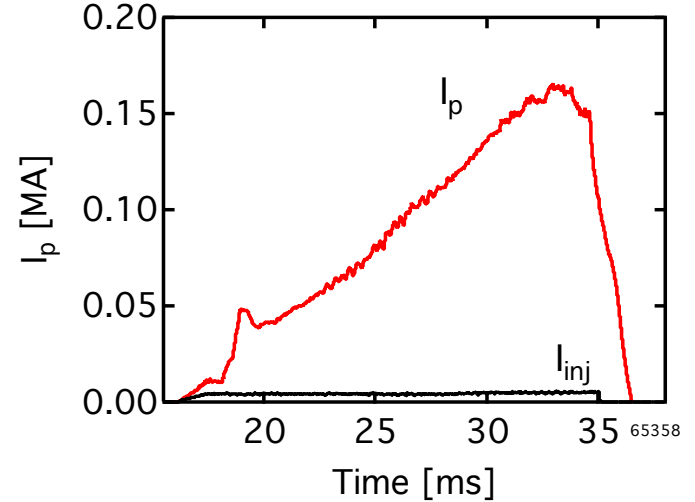


Outboard LHI Provides Robust Startup on the PEGASUS ST

Helicity Injectors



$I_p \leq 0.18$ MA via LHI ($I_{inj} = 5$ kA)



Plasma

Parameters

$I_p \leq 0.23$ MA
 $\tau_{shot} \leq 0.025$ s
 $B_T = 0.15$ T
 $A = 1.15-1.3$
 $R = 0.2-0.45$ m
 $a \leq 0.4$ m
 $\kappa = 1.4-3.7$

Parameters

$\sum I_{inj} \leq 14$ kA
 $I_{inj} \leq 2$ kA
 $V_{inj} \leq 2.5$ kV
 $N_{inj} \leq 4$
 $A_{inj} = 2$ cm²
 $I_{arc} \leq 2$ kA
 $V_{arc} \leq 0.5$ kV

Injector

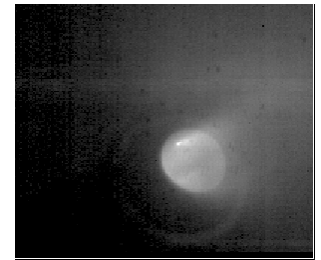
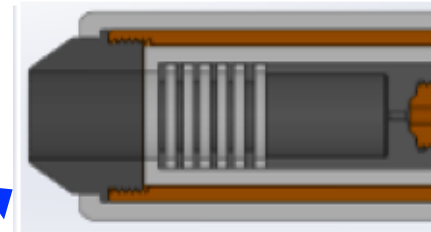
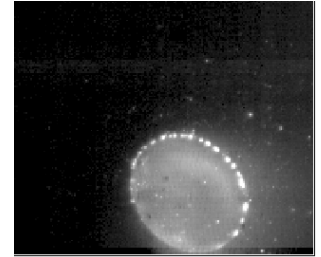
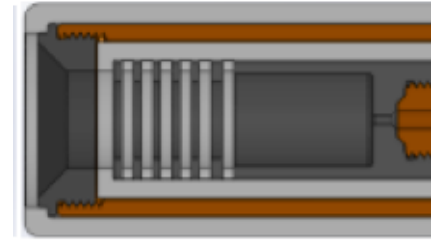


Controlling Plasma-Material Interaction is Enabling High V_{INJ} Operation

- Injector requirements include

- Large $A_{\text{inj}}, J_{\text{inj}}$
- $V_{\text{inj}} > 1 \text{ kV}$
- $\Delta t_{\text{pulse}} \sim 10\text{-}100 \text{ ms}$
- Minimize PMI

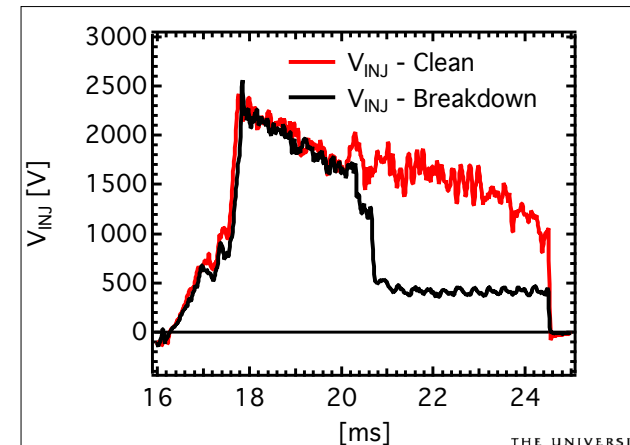
...all adjacent to tokamak LCFS



- Advanced injector design enables high V_{inj}

- Cathode shaping to mitigate cathode spots
- Shielding of cathode, insulators to prevent injector breakdown
- 3x improvement in $V_{\text{inj}}, \Delta t_{\text{pulse}}$

Voltage of quiescently operating injectors (red) and voltage after breakdown of overdriven injectors (black)



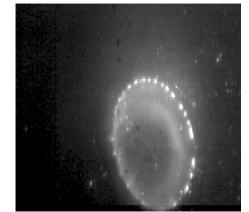
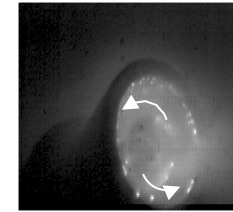
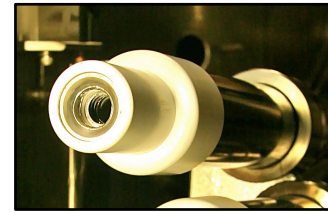


Technology & Science Challenges for NSTX-U & Beyond

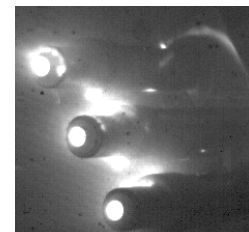
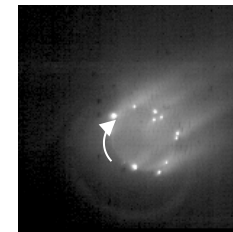
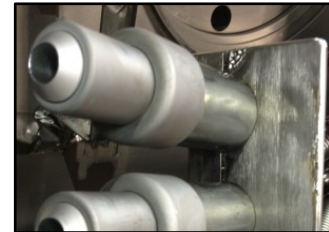
- Long-pulse startup (100ms)
 - Injector heat load
 - Edge density control
 - Plasma control
- High B_{TF}
 - Confinement scaling
 - Effective injector size
 - Initial tokamak formation
 - Reconnection with high guide field
- Close fitting wall
 - Potentially complicates relaxation

Injector technology evolving to meet physics challenges

Concave cathode: Cathode spots near BN \rightarrow PMI

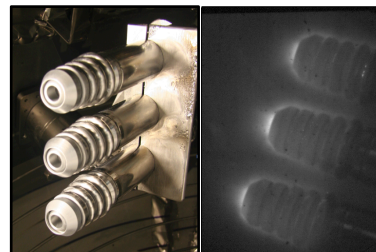


Frustum cathode, local limiter:



Cathode spot control, but arc-back

Stepped shielding: Mitigate spots & arc-back, but heat-load cracking



Spore-node, shield rings



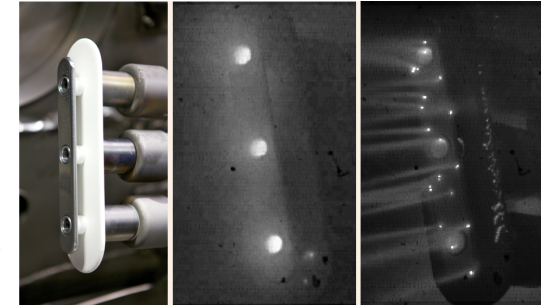


Tests of Various Injector Concepts Favor Smaller A_{INJ} , High V_{INJ}

- Tests of large-area passive electrodes show reduced effective A_{INJ}

- Integrated metallic electrode surface

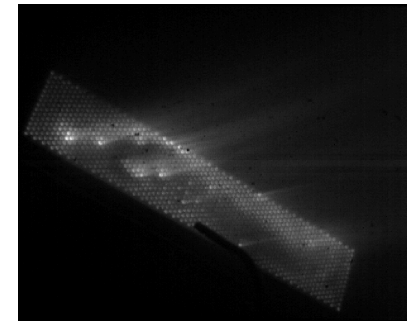
- Cathode spot emission



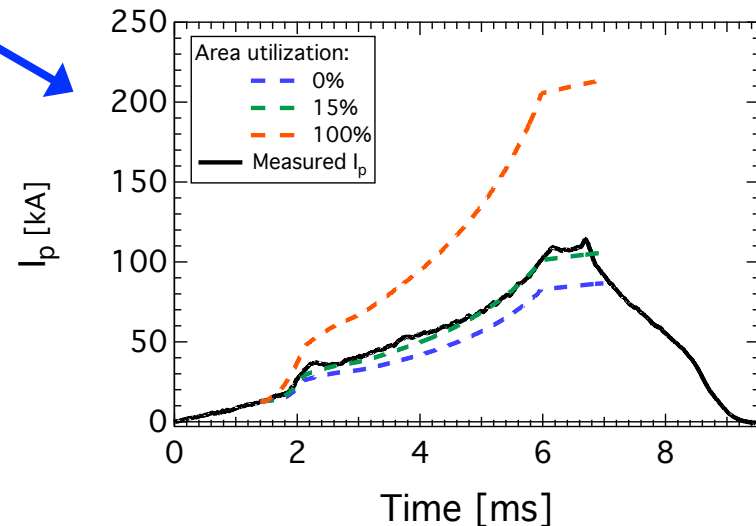
Above: integrated electrode injector assembly

- Large area gas-effused Mo Plate

- Hollow cathode emission
- Non-uniform J_{INJ} , effective $A_{INJ} = 0.15 A_{GEOMETRIC}$

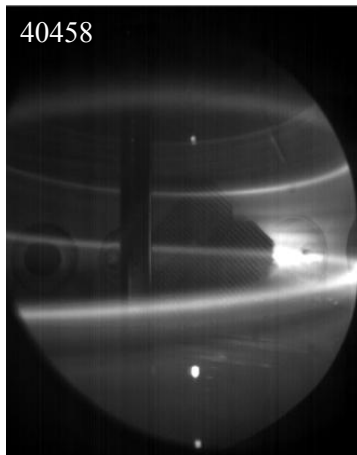
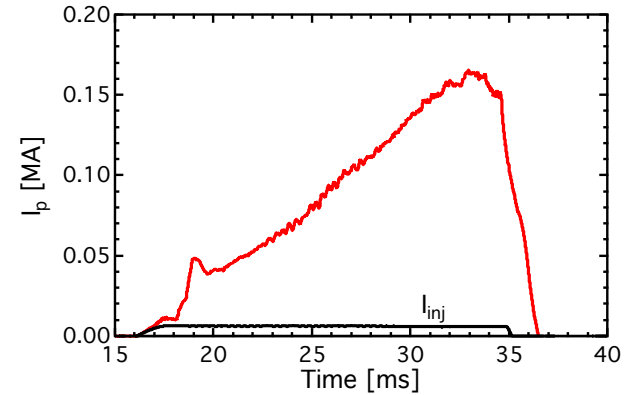
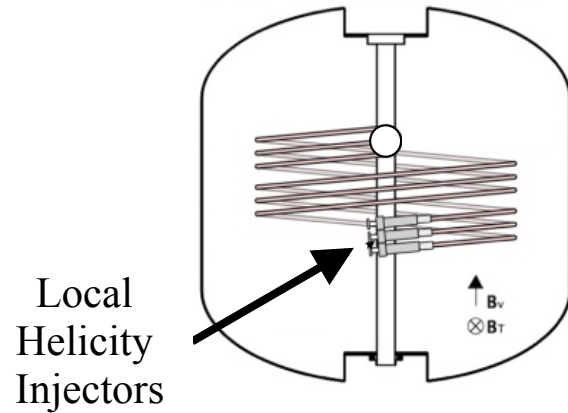


- Conclusion: Arc-based injector system most effective path to maximize HI rate





LHI Injects Current Streams that Relax, Form Tokamak-Like Plasma

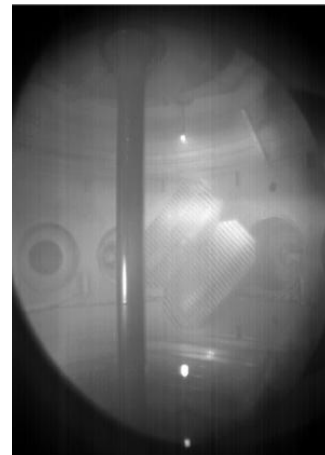


Force-free current streams

Null Formation

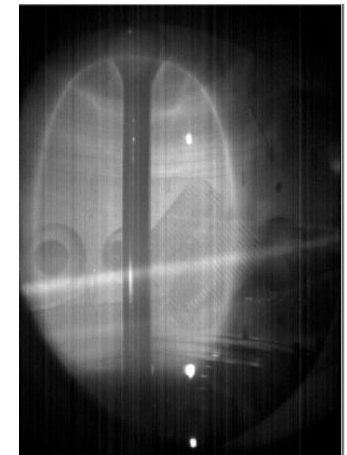


Relaxation



Tokamak-like state

Injector Shutoff



Tokamak forms



Helicity Balance, Taylor Relaxation Criteria Set Max Achievable I_p from LHI

Helicity balance in a Tokamak geometry:

$$\frac{dK}{dt} = -2 \int_V \eta \mathbf{J} \cdot \mathbf{B} d^3x - 2 \frac{\partial \psi}{\partial t} \Psi - 2 \int_A \Phi \mathbf{B} \cdot d\mathbf{s} \quad \longrightarrow \quad I_p \leq \frac{A_p}{2\pi R_0 \langle \eta \rangle} (V_{ind} + V_{eff})$$

- Helicity injection provides an effective loop voltage^{*,**}:

$$V_{eff} \approx \frac{A_{inj} B_{\phi, inj}}{\Psi_T} V_{inj}$$

Taylor relaxation of a force-free equilibrium:

$$\begin{aligned} \nabla \times \mathbf{B} = \mu_0 \mathbf{J} = \lambda \mathbf{B} \\ \langle \lambda_p \rangle \leq \langle \lambda_{edge} \rangle \end{aligned} \quad \longrightarrow \quad \frac{\mu_0 I_p}{\Psi_T} \leq \frac{\mu_0 I_{inj}}{2\pi R_{inj} w B_{\theta+V, inj}} \quad \xrightarrow{**} \quad I_p \leq \sqrt{\frac{1}{B_{\theta+V, inj} / I_p} \frac{\Psi_T I_{inj}}{2\pi R_{inj} w_{inj}}}$$

| | | | |
|-----------|-------------------------------|---------------------|---------------------------------------|
| A_p | Plasma area | Ψ_T | Plasma toroidal flux |
| w_{inj} | Edge current channel width | $B_{\theta+V, inj}$ | Poloidal field in injection region |

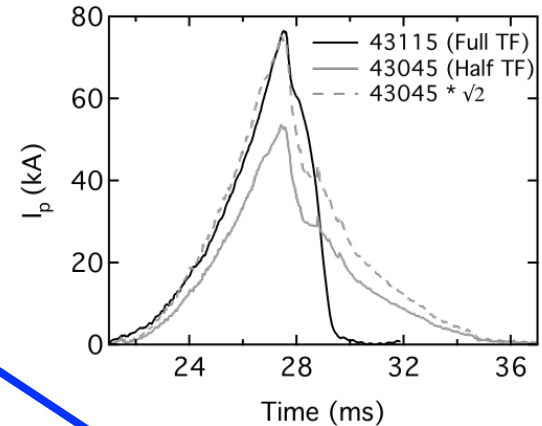
*D.S. Darrow, *et al. Physics of Fluids B: Plasma Physics*, 2(6): 1415, 1990.

**D.J. Battaglia. *Non-solenoidal tokamak startup using localized current sources near the outboard midplane*. PhD thesis, UW-Madison, 2009.

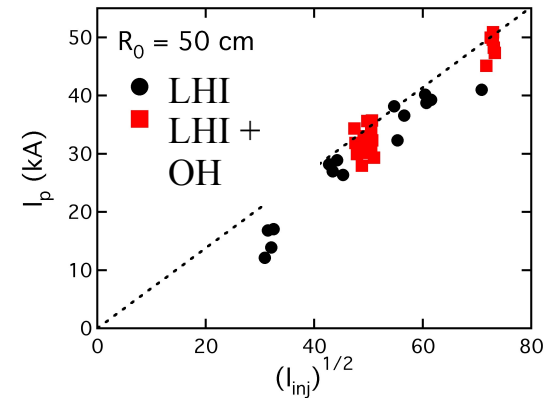
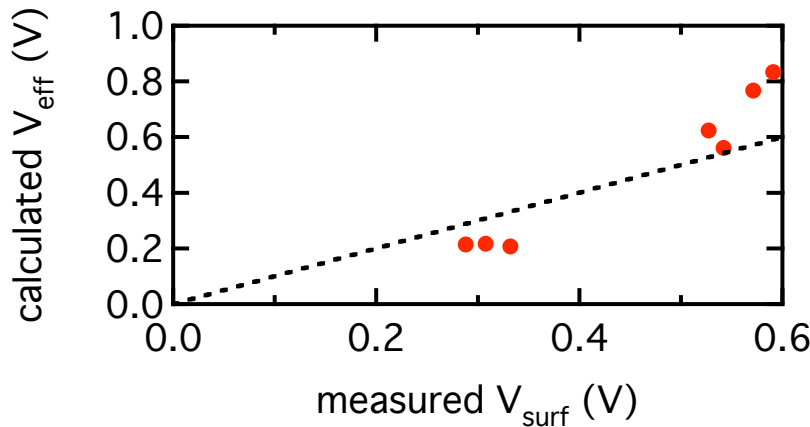


Global Helicity Balance, Taylor Relaxation Limits Confirmed

- At Taylor Limit: $I_p^{\max} \propto \sqrt{I_{INJ}}, \sqrt{I_{TF}}, W^{-1/2}$



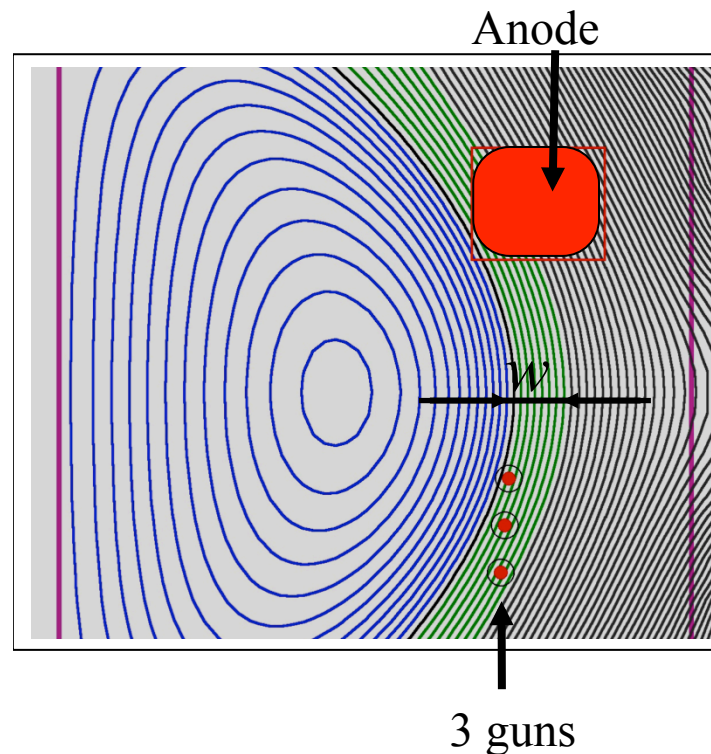
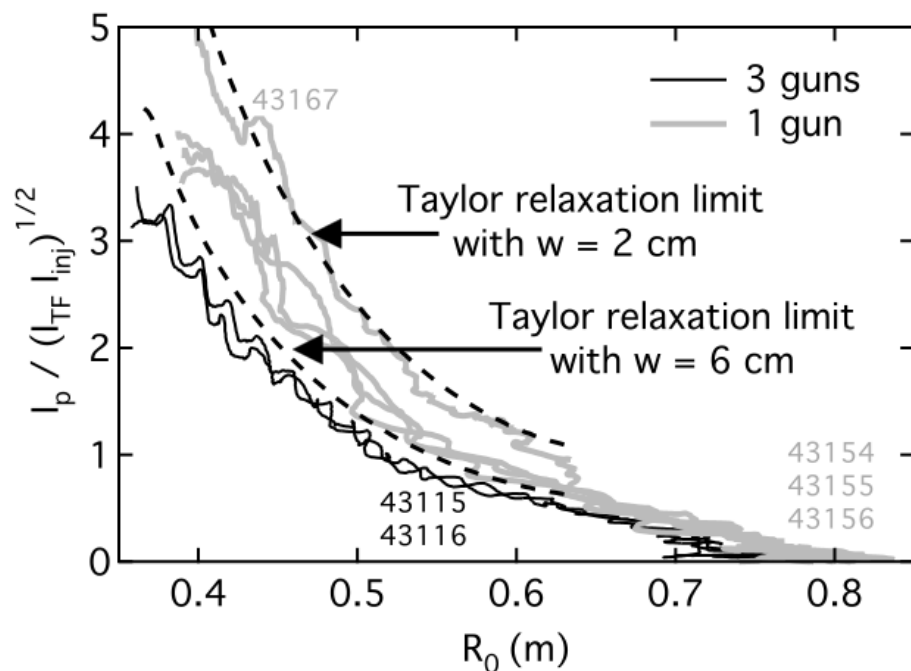
- V_{eff} agreement over limited data set





Experiments demonstrate dependence on the width of the driven current layer

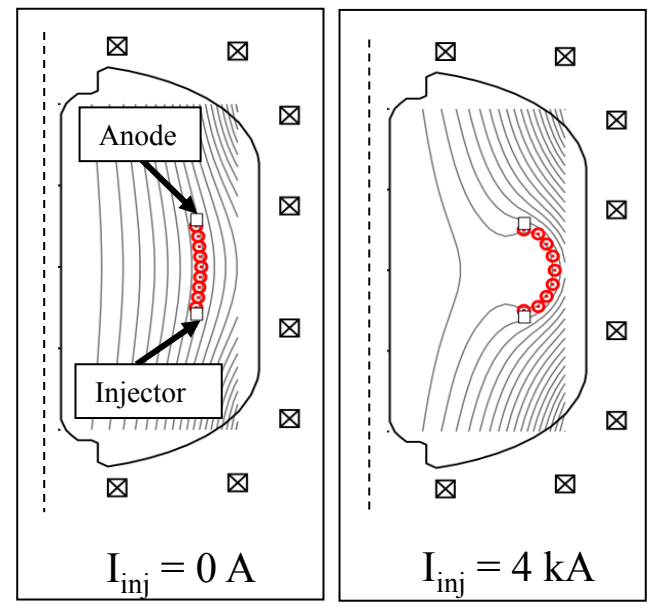
- Relaxation current limit scales as $w^{-1/2}$
- One-gun discharges had higher limits than corresponding three-gun cases, indicating the gun array was misaligned:



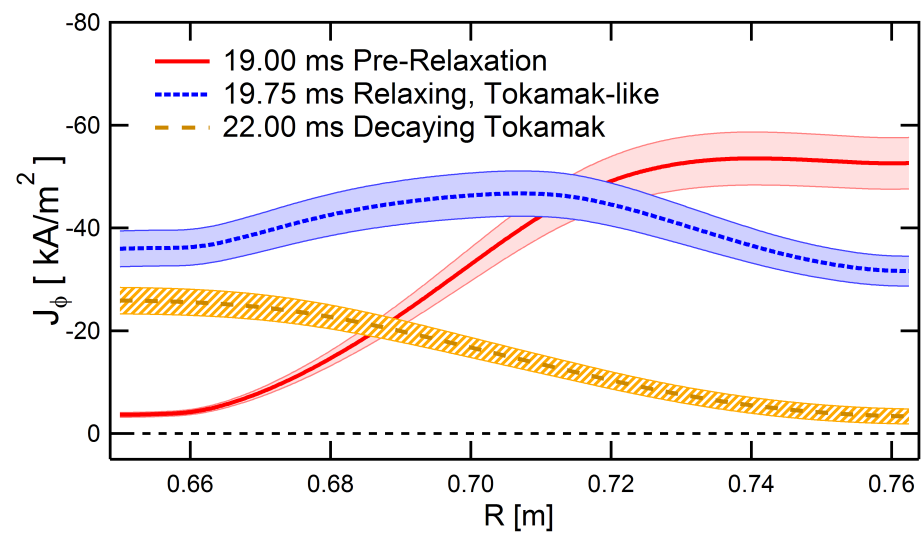
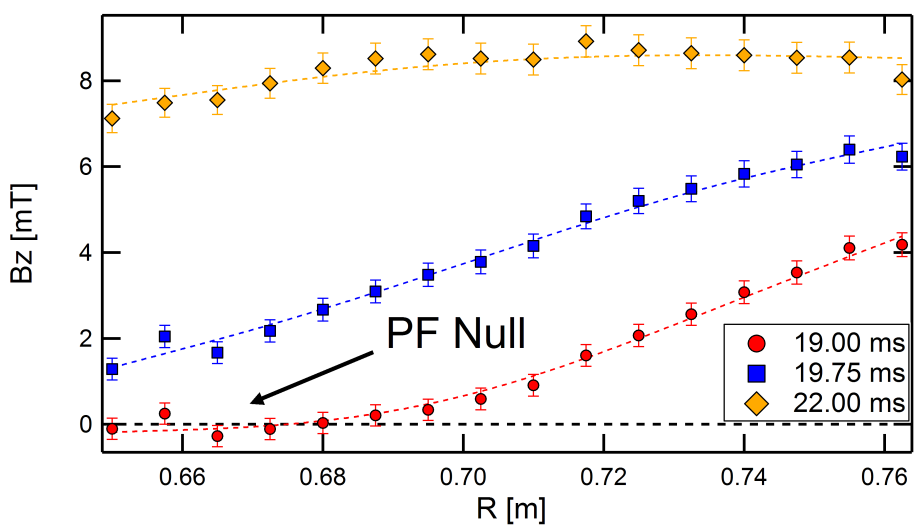


Internal Measurements Show Null Formation, $J(R,t)$ Throughout LHI Discharge Evolution

- Initial relaxation to tokamak-like topology coincident with inboard null formation
 - Injected current filaments perturb vacuum \mathbf{B}
 - B_z must be sufficiently low and/or I_{inj} sufficiently high for null to form
- Hall probe* $B_z(R)$ provides $J_\phi(R)$ evolution
 - Predicted field null observed



*: Bongard *et al.*, Rev. Sci. Instrum. **81**, 10E105 (2010)





2. When $I_p(t) < \text{Taylor Limit 0-D Power Balance Model Predicts } I_p(t)$

- Lumped parameter model + helicity conservation:

$$I_p \left[\underbrace{V_{eff}}_{\text{blue}} + \underbrace{V_R}_{\text{red}} + \underbrace{V_{PF}}_{\text{green}} + \underbrace{V_{Lp}}_{\text{purple}} \right] = 0$$

- V_{eff} : From **helicity injection**
 - V_R : **Resistive dissipation** from assumed flat Spitzer $T_e(R,t) = 70\text{eV}$
 - V_{PF} : **Poloidal induction** voltage
 - V_{Lp} : Voltage due to **plasma self-inductance**
- Inputs: $R_0(t)$, $a(t)$, $I_p(t_0)$, $\langle \eta_0 \rangle$, $\kappa(t)$, $\ell_i(t)$
 - Analytic low-A descriptions of L_p , B_z , plasma shape
 - Differential equation in $I_p(t)$ solved when $I_p(t) < I_{\text{Taylor}}(t)$



Poynting's Theorem Applied at Plasma Boundary Defines Current Sources & Sinks

$$\underline{I_p V_s} = \underline{\iiint \frac{\partial}{\partial t} \left(\frac{B_\theta^2}{2\mu_0} \right) dV} + \underline{I_p^2 R_p} - \underline{I_p V_{NICD}}$$

Plasma surface voltage

- Inductive drive from OH, PF-ramping
- Self-inductance: contribution from *external* fields

$$\underline{V_s} = - \frac{\partial}{\partial t} \left(\psi_{OH} + \sum_i \psi_{PF,i} + L_e I_p \right)$$

Internal magnetic energy

- Self-inductance: contribution from *internal* fields, static boundary

$$\underline{\frac{1}{I_p} \frac{\partial}{\partial t} (W_{B,p})} = \frac{1}{I_p} \frac{\partial}{\partial t} \left(\frac{1}{2} L_i I_p^2 \right)$$

Resistive dissipation

- Uniform, constant Spitzer resistivity assumed

$$\underline{V_R} = I_p R_p = I_p \left(\frac{\langle \eta_p \rangle 2\pi R_0}{A_p} \right)$$

Non-inductive current drive

- Local helicity injection

$$\underline{V_{NICD}} = V_{eff} \approx \frac{A_{inj} B_{\phi,inj}}{\Psi_T} V_{inj}$$



Plasma Self-Inductance Modeled with Analytic, Low-A Approximations

- Plasma self-inductance is partitioned into internal, external components:

$$L_p = \underline{L_i} + \underline{L_e}$$

- External component L_e is heavily aspect-ratio dependent:

$$\underline{L_e} = \mu_0 R_0 \frac{a(\varepsilon)(1-\varepsilon)}{1-\varepsilon + \kappa b(\varepsilon)}$$

where $\varepsilon = \frac{1}{A}$

$$a(\varepsilon) = \left(1 + 1.81\sqrt{\varepsilon} + 2.05\varepsilon\right) \ln\left(\frac{8}{\varepsilon}\right) - \left(2.0 + 9.25\sqrt{\varepsilon} + 1.21\varepsilon\right)$$

$$b(\varepsilon) = 0.73\sqrt{\varepsilon} \left(1 + 2\varepsilon^4 - 6\varepsilon^5 + 3.7\varepsilon^6\right)$$

*S.P. Hirshman and G.H. Nielson 1986 *Phys. Fluids* **29** 790

- Internal component decreasing in time (typically $\ell_i = 0.5 \rightarrow 0.2$):

$$W_{B,p} = \underbrace{\iiint_{V_p} \frac{B_\theta^2}{2\mu_0} dV}_{\underline{\quad}} = \frac{1}{2} \underline{L_i} I_p^2 = \frac{1}{2} \left(\underbrace{\frac{\mu_0 V_p}{C_p^2} \ell_i}_{\underline{\quad}} \right) I_p^2$$



Plasma Self-Inductance Modeled with Analytic, Low-A Approximations

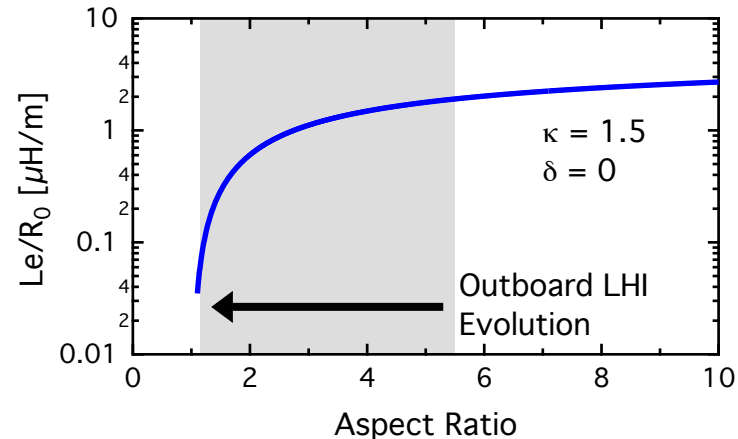
- Plasma self-inductance is partitioned into internal, external components:

$$L_p = \underline{L_i} + \underline{L_e}$$

- External component L_e is heavily aspect-ratio dependent:

$$\underline{L_e} = \mu_0 R_0 \frac{a(\varepsilon)(1-\varepsilon)}{1-\varepsilon + \kappa b(\varepsilon)}$$

where $\varepsilon = \frac{1}{A}$



- Internal component decreasing in time (typically $\ell_i = 0.5 \rightarrow 0.2$):

$$W_{B,p} = \iiint_{V_p} \frac{B_\theta^2}{2\mu_0} dV = \frac{1}{2} \underline{L_i} I_p^2 = \frac{1}{2} \left(\frac{\mu_0 V_p}{C_p^2} \ell_i \right) I_p^2$$



Low- A , Analytic Models Approximate V_{PF}

- Applied vertical field provides force-balance and inductive loop-voltage
 - Ψ_{PF} estimated with Hirshman & Nielson* mutual inductance-like M_v equation

$$\underline{V_{PF}} = \frac{\partial}{\partial t} \left(\sum_i \psi_{PF,i} \right) \approx \frac{\partial}{\partial t} \left[M_v \pi R_0^2 B_v |_{R_0} \right]$$

where
$$M_v(\epsilon, \kappa) = \frac{(1-\epsilon)^2}{(1-\epsilon)^2 c(\epsilon) + d(\epsilon)\sqrt{\kappa}}$$

$$c(\epsilon) = 1 + 0.98\epsilon^2 + 0.49\epsilon^4 + 1.47\epsilon^6$$

$$d(\epsilon) = 0.25\epsilon(1 + 0.84\epsilon - 1.44\epsilon^2)$$

*S.P. Hirshman and G.H. Nielson 1986 *Phys. Fluids* **29** 790

- B_v required for force-balance is aspect-ratio and shape dependent
 - Uses Mitarai & Takase* formula for B_v for force-balance at low- A with κ :

$$B_v = \frac{\mu_0 I_p}{4\pi R_0} \left\{ \frac{1}{\mu_0} \frac{\partial L_e}{\partial R} + \frac{\ell_i}{2} + \beta_p - \frac{1}{2} \right\}$$

*O. Mitarai and Y. Takase 2003 *Fusion Sci. Technol.*



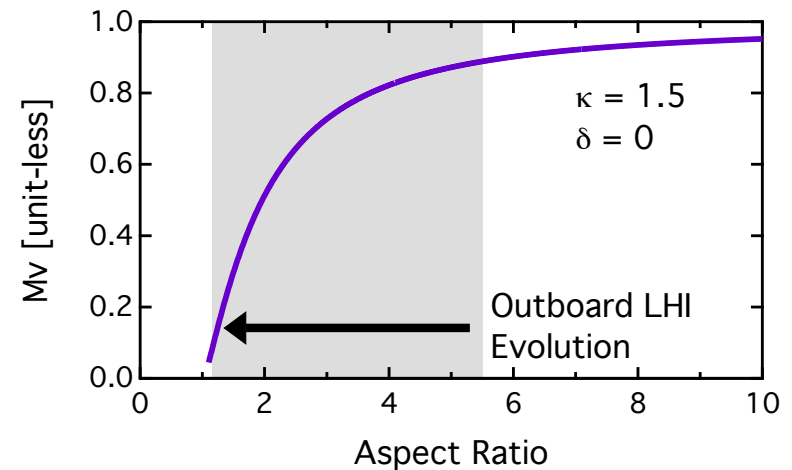
Low-A, Analytic Models Approximate V_{PF}

- Applied vertical field provides force-balance and inductive loop-voltage
 - Ψ_{PF} estimated with Hirshman & Nielson* mutual inductance-like M_v equation

$$\underline{V_{PF}} = \frac{\partial}{\partial t} \left(\sum_i \psi_{PF,i} \right) \approx \frac{\partial}{\partial t} \left[M_v \pi R_0^2 B_v |_{R_0} \right]$$

where

$$M_v(\epsilon, \kappa) = \frac{(1-\epsilon)^2}{(1-\epsilon)^2 c(\epsilon) + d(\epsilon) \sqrt{\kappa}}$$



- B_v required for force-balance is aspect-ratio and shape dependent
 - Uses Mitarai & Takase* formula for B_v for force-balance at low-A with κ :

$$B_v = \frac{\mu_0 I_p}{4\pi R_0} \left\{ \frac{1}{\mu_0} \frac{\partial L_e}{\partial R} + \frac{\ell_i}{2} + \beta_p - \frac{1}{2} \right\}$$

*O. Mitarai and Y. Takase 2003 *Fusion Sci. Technol.*



System Represented by ODE Initial Value Problem

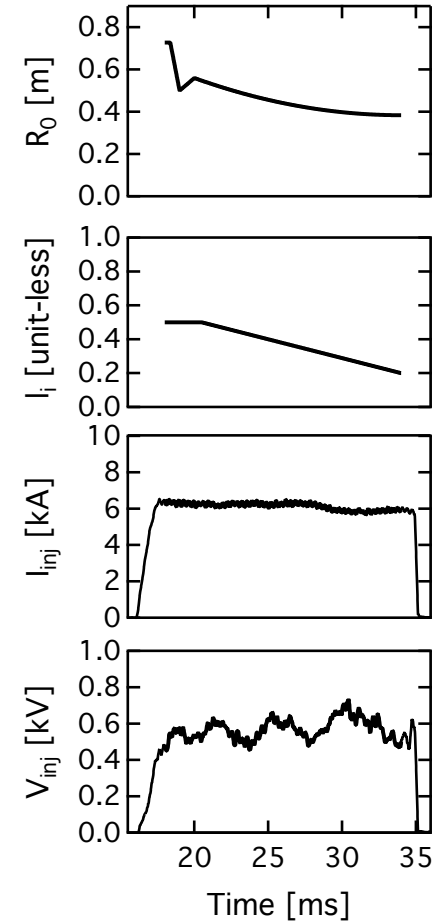
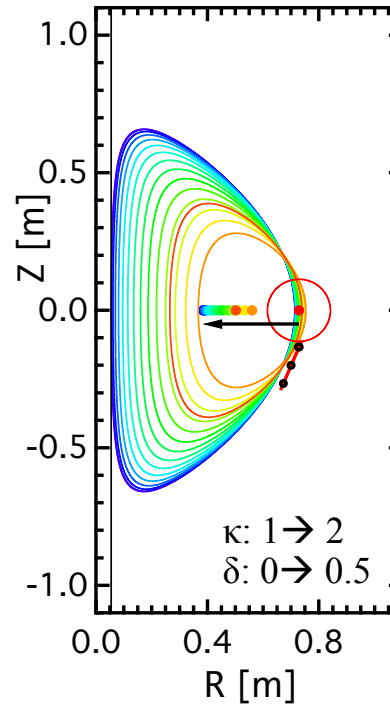
$$\frac{\partial I_p}{\partial t} = - \frac{\frac{1}{2} \frac{\partial L_i}{\partial t} + \frac{\partial L_e}{\partial t} + R_p + \frac{\partial}{\partial t} \left[M_v \pi R_0^2 \left(\frac{B_v}{I_p} \right) \right]}{L_p + M_v \pi R_0^2 \left(\frac{B_v}{I_p} \right)} I_p + \frac{V_{OH} + V_{eff}}{L_p + M_v \pi R_0^2 \left(\frac{B_v}{I_p} \right)}$$

- At initial relaxation to tokamak-like state:
 - Initial value from Taylor limit
- If $I_{p, \text{Pow. Bal.}} > I_{p, \text{Taylor}}$: follow Taylor limit
- Else: follow power-balance



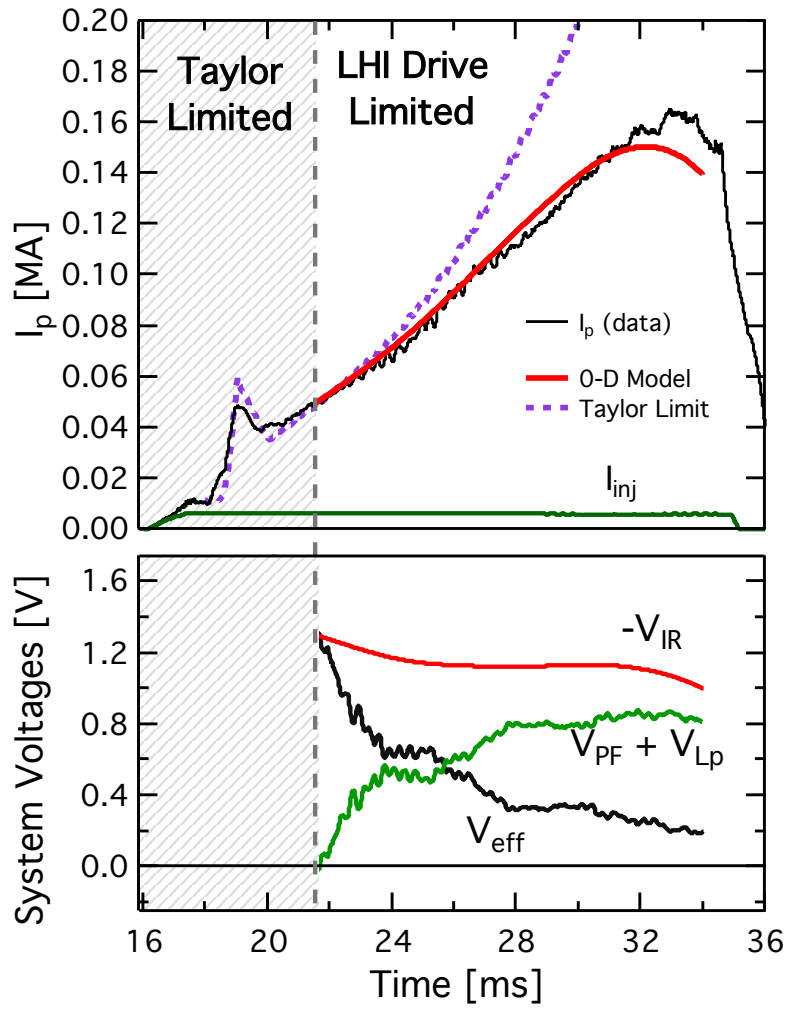
Plasma Parameters Constitute Power-Balance Inputs

- $I_p(t_0)$
 - Initial condition to DE solver
- Shape
 - $R_0(t)$, $a(t)$, $\kappa(t)$, $\delta(t)$
- Plasma parameters
 - $\langle \eta \rangle$ assumed constant, Spitzer
 - $\beta_p = 0$
 - ℓ_i : $0.5 \rightarrow 0.2$
- LHI parameters
 - $A_{inj}(t)$, $V_{inj}(t)$





LHI Plasmas Undergo Two-Phase $I_p(t)$ Evolutions

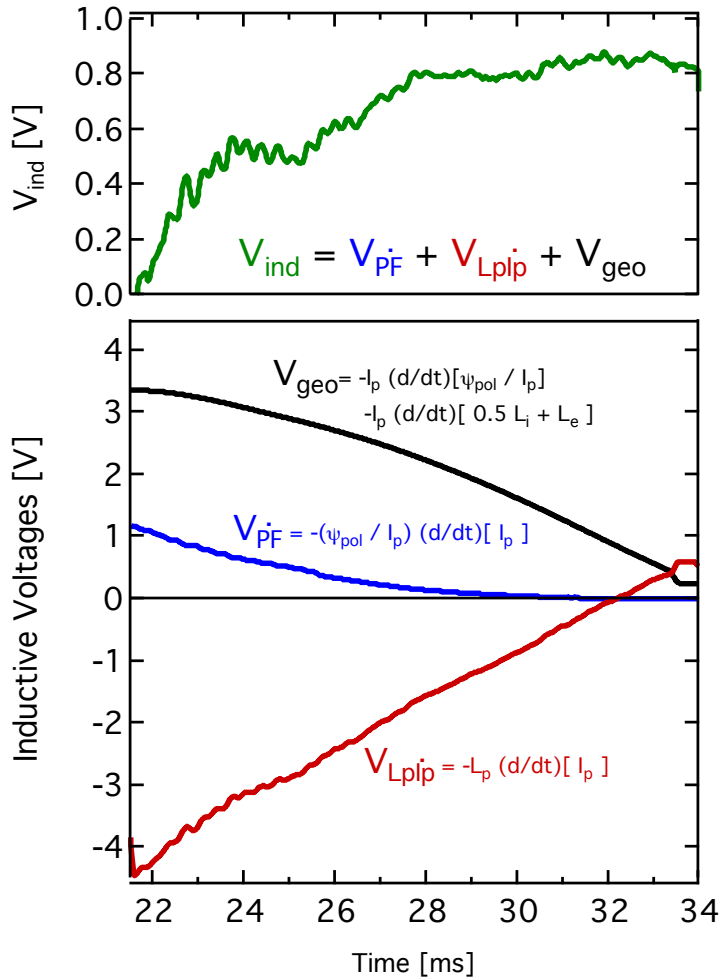


- Low I_p : Taylor limited
 - Set by plasma geometry, I_{inj}

- Higher I_p : power-balance
 - Balance of LHI, inductive effects, resistive losses



Using 0-D Model as Interpretive Tool Gives Insight into LHI Current Dynamics



- Inductive voltages dominated by geometric evolution
- Geometry evolution ~ 3 V
- PF ramping ~ 1 V
- Inductive reactance ~ 4 V



Testing and Calibration of the Model Proceeding on Multiple Fronts

$$\underline{I_p V_s} = \frac{\partial}{\partial t} (\underline{W_{B,p}}) + \underline{I_p^2 R_p} - \underline{I_p V_{NICD}}$$

- $I_p(t)$ compared for various plasma evolutions

Plasma surface voltage

$$\underline{V_s} = - \frac{\partial}{\partial t} \left(\psi_{OH} + \sum_i \psi_{PF,i} + L_e I_p \right)$$

Internal magnetic energy

$$\underline{\frac{1}{I_p} \frac{\partial}{\partial t} (W_{B,p})} = \frac{1}{I_p} \frac{\partial}{\partial t} \left(\frac{1}{2} L_i I_p^2 \right)$$

Resistive Dissipation

$$\underline{V_R} = I_p R_p = I_p \left(\frac{\eta_p 2\pi R_0}{A_p} \right)$$

Non-inductive current drive

$$\underline{V_{NICD}} = V_{eff}$$

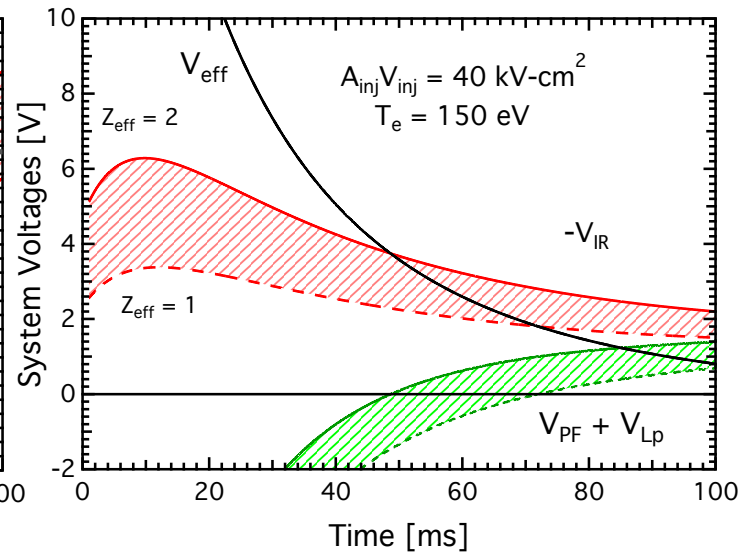
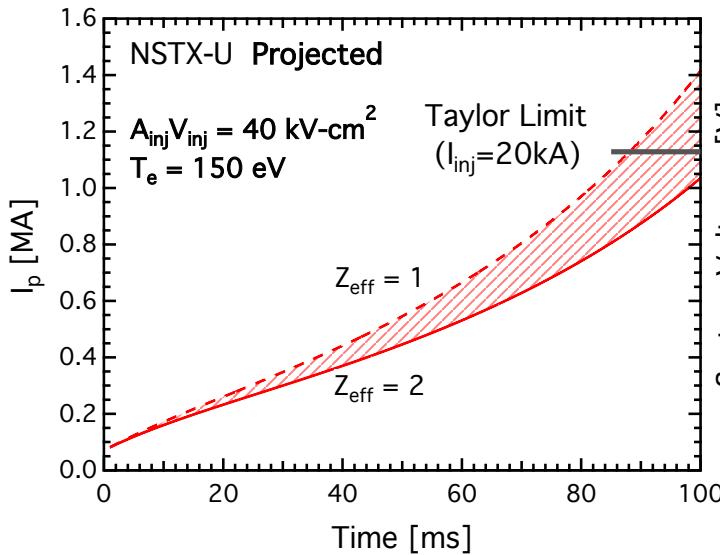
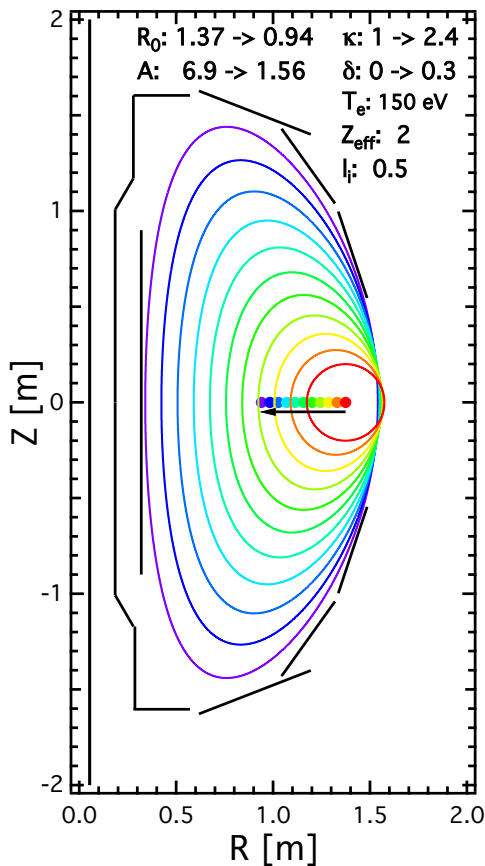
- Approximations for $\psi_s(t)$, $W_m(t)$, $L_i(t)$ calibrated to experiment

- Thomson Scattering
- TF variations

- Upgraded injector systems to vary V_{eff}



Model Applied to NSTX-U Geometry for Initial $I_p \sim 1$ MA Start-up Scenario Prediction



- Significant LHI drive required to achieve $I_p \sim 1$ MA
 - Predicted $A_{\text{inj}} V_{\text{inj}}$ requirement estimates: $\sim 40 \text{ cm}^2\text{-kV}$

*C. Neumeyer *et al* (2009) 23rd IEEE/NPSS Symposium on Fusion Engineering

**C. Neumeyer (2001) "NSTX Internal Hardware Dimensions"

http://nstx.pppl.gov/nstx/Engineering/NSTX_Eng_Site/Technical/Machine/NSTX_Eng_Machine_Dims_cm.html



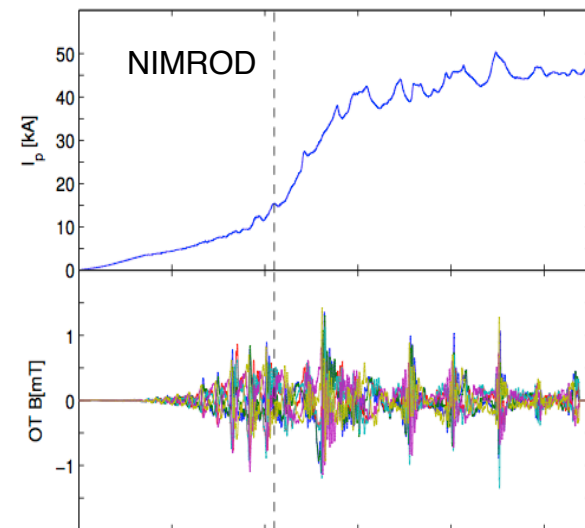
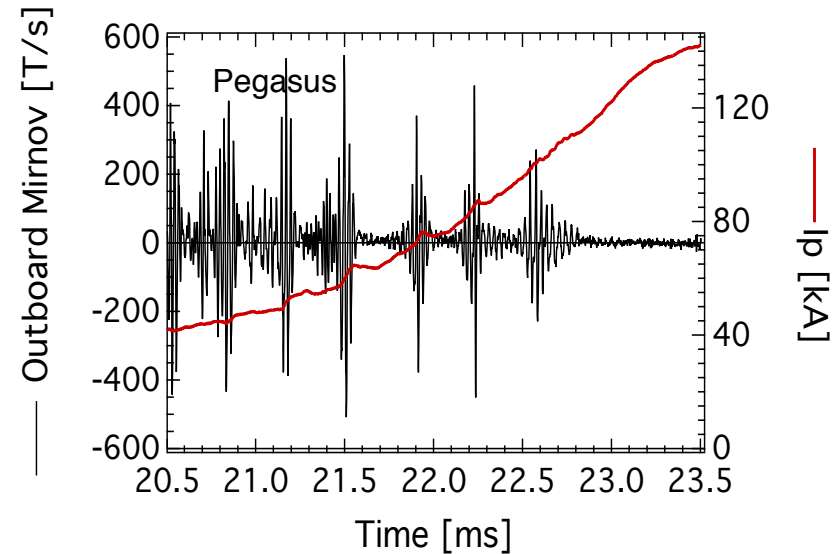
Current Growth During LHI Correlated with Bursts of MHD Activity

Measured burst properties include

- Two primary spectral components
 - $n=1 \Rightarrow 10\text{-}20\text{kHz}$ @ R_{inj} , line-tied
 - $n=0 \Rightarrow <5\text{ kHz}$, plasma motion
- Typically correlates with sharp I_p increase

NIMROD simulations produce bursty MHD

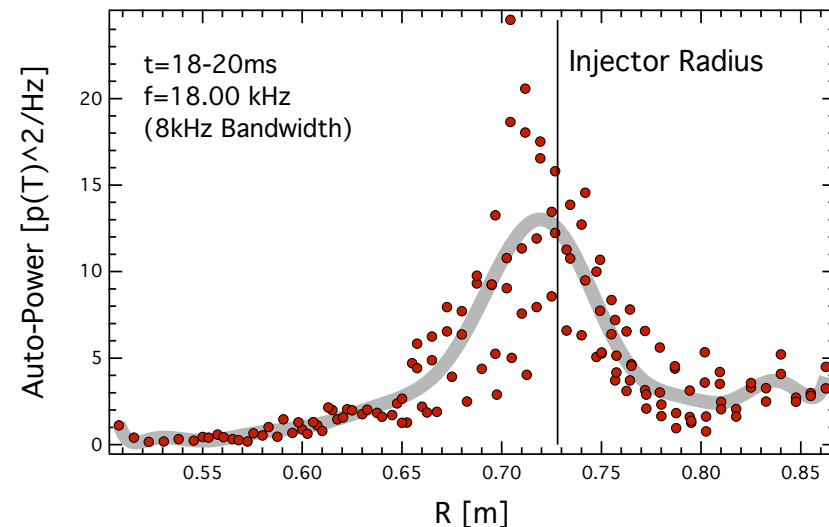
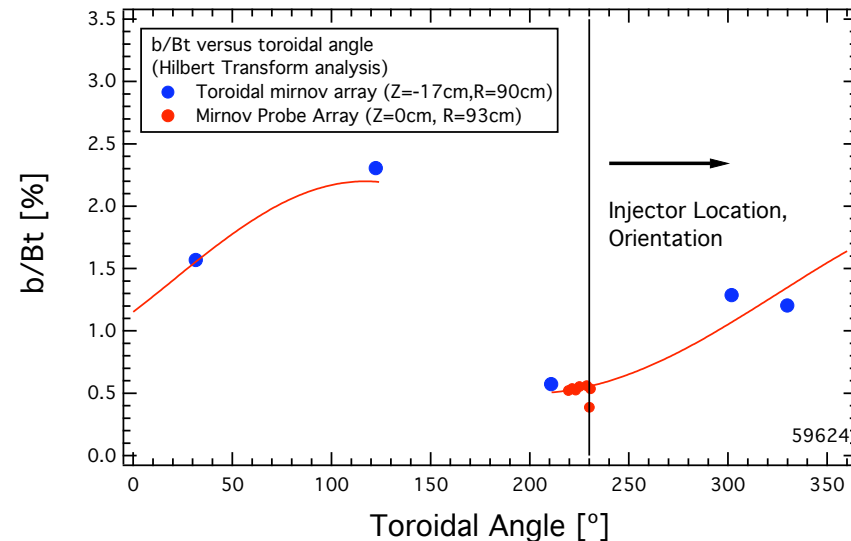
- Bursts from transient reconnection events
- Qualitative agreement with experiment





Bursts show $n=1$

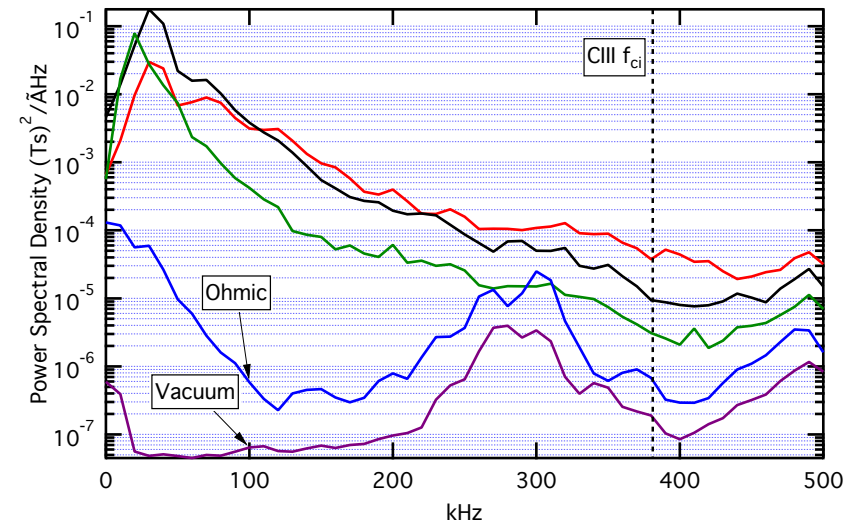
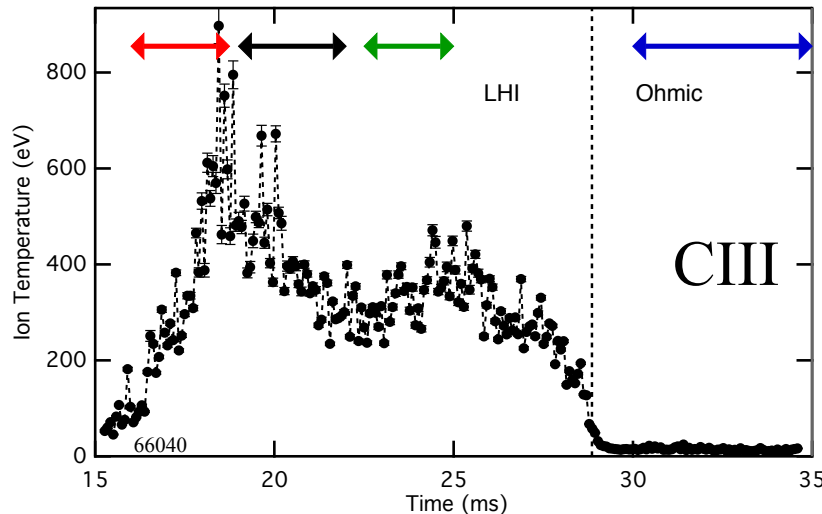
- Current multiplication, transport accompanied by MHD activity
- Two common spectral features
 - High-frequency 10–20 kHz $n = 1$
 - Low-frequency < 5 kHz $n = 0$
- $n = 1$ mode consistent with line tying
 - Activity localized near injector radius
 - Toroidal asymmetry in
- $n = 0$ localized to plasma interior
 - Inward radial motion





Potential Reconnection-Induced Impurity Ion Heating Observed during LHI

- NIMROD shows magnetic reconnection during LHI
 - Ion heating commonly observed in reconnection experiments*
- Consistent with ion cyclotron heating mechanism**
 - Pegasus LHI MHD spectra show significant power in IC resonance region



*: Magee, *et al.* Phys. Rev. Let. **107**, 065005 (2011)

** : Tangri



Predictive Understanding of Plasma Impedance Required for Projecting to Higher I_p

- Determines feasible V_{INJ} , A_{INJ} , I_{INJ} and demands on power system
- Governed by plasma physics of arc source and tokamak edge
 - Low I_{INJ} : Double layer $J_{INJ} \sim V_{INJ}^{3/2}$
 - High I_{INJ} : Space charge neutralization of e-beam by edge plasma

$$J_{INJ} = n_{edge} e \sqrt{\frac{2e}{m_e}} \sqrt{V_{INJ}}$$

- n_{edge} dependence to be validated
 - Assuming $n_{edge} \sim$ fill pressure

Ramp-up I-V characteristics for Pegasus injectors agrees with 2-parameter model across wide range of fill pressures

